Use of quadrupolar nuclei for quantum-information processing by nuclear magnetic resonance: Implementation of a quantum algorithm

Ranabir Das[1] and Anil Kumar[1,2]
[1]*Department of Physics, Indian Institute of Science, Bangalore 560012, India*
[2]*Sophisticated Instruments Facility, Indian Institute of Science, Bangalore 560012, India*
(Received 26 December 2002; published 10 September 2003)

Physical implementation of quantum-information processing by liquid-state nuclear magnetic resonance, using weakly coupled spin-$\frac{1}{2}$ nuclei of a molecule, is well established. Nuclei with spin$>1/2$ oriented in liquid-crystalline matrices is another possibility. Such systems have multiple qubits per nuclei and large quadrupolar couplings resulting in well separated lines in the spectrum. So far, creation of pseudopure states and logic gates has been demonstrated in such systems using transition selective radio-frequency pulses. In this paper we report two developments. First, we implement a quantum algorithm that needs coherent superposition of states. Second, we use evolution under quadrupolar coupling to implement multiqubit gates. We implement the Deutsch-Jozsa algorithm on a spin-$\frac{3}{2}$ (2 qubit) system. The controlled-NOT operation needed to implement this algorithm has been implemented here by evolution under the quadrupolar Hamiltonian. To the best of our knowledge, this method has been implemented for the first time in quadrupolar systems. Since the quadrupolar coupling is several orders of magnitude greater than the coupling in weakly coupled spin-$\frac{1}{2}$ nuclei, the gate time decreases, increasing the clock speed of the quantum computer.

DOI: 10.1103/PhysRevA.68.032304 PACS number(s): 03.67.Lx

I. INTRODUCTION

In 1985 Deutsch suggested an algorithm that demonstrated the use of ''massive quantum parallelism'' inherent in quantum systems [1]. Better known as the Deutsch-Jozsa (DJ) algorithm, it can distinguish between a ''constant'' and a ''balanced'' function in an N-qubit system in one function call, whereas its classical counterpart requires on average $(2^{N-1}+1)$ function calls [1,2]. Over the years, quantum-information processing has been demonstrated in various physical systems [3,4]. Nuclear magnetic resonance (NMR) has also successfully demonstrated several avenues of quantum-information processing [5–25]. Quantum algorithms such as the Deutsch-Jozsa algorithm, Grover's search algorithm, and Shor's prime factorization algorithm have been successfully implemented by liquid state NMR using molecules having weakly coupled spin-$\frac{1}{2}$ nuclei [10–18]. In such systems each nucleus is identified as a qubit and the coupling between the qubits (nuclei) is mediated through covalent bonds (indirect spin-spin J coupling).

A growing appreciation among researcher's is the use of quadrupolar nuclei with spin$>\frac{1}{2}$ as a suitable candidate for quantum-information processing [20–25]. The energy levels of a quadrupolar nucleus are equispaced in a liquid, yielding degenerate single quantum NMR transitions. This degeneracy is lifted in a liquid-crystalline matrix yielding $2I$ well resolved transitions, allowing the $2I+1$ eigenstates of a half-integer spin I nucleus to be treated as states of an N-qubit system, provided $(2I+1)=2^N$. In such cases a single quadrupolar nucleus acts as several qubits [21]. In such systems, while the quadrupolar splittings are of the order of several kHz, the linewidths are only of few Hertz. Short and precise transition selective pulses can be applied to such systems [21,24].

The Hamiltonian of a quadrupolar nucleus partially oriented in a liquid-crystalline matrix, in the presence of a large magnetic field B_0 and having a first-order quadrupolar coupling, is given by [26]

$$\begin{aligned}\mathcal{H} &= \mathcal{H}_Z + \mathcal{H}_Q \\ &= -\omega_0 I_z + \frac{e^2qQ}{4I(2I-1)}(3I_z^2 - I^2)S \\ &= -\omega_0 I_z + \Lambda(3I_z^2 - I^2), \end{aligned} \tag{1}$$

where $\omega_0=\gamma B_0$ is the resonance frequency, γ being the gyromagnetic ratio, S is the order parameter at the site of the nucleus, e^2qQ is the quadrupolar coupling, and $\Lambda = e^2qQS/[4I(2I-1)]$ is the effective quadrupolar coupling. Though e^2qQ is of the order of several MHz, a small value for the order parameter S converts the effective quadrupolar coupling Λ into several kHz. Preparation of pseudopure states, implementation of logic gates, and half-adder/subtracter operations and quantum simulations have already been demonstrated in such systems [21–25]. However, so far only logical operations that do not require coherent superposition have been implemented in such systems. In this work, we demonstrate that such systems can also be utilized for quantum-information processing by implementing algorithms that need coherent superpositions of states such as the Deutsch-Jozsa (DJ) algorithm. Moreover, we propose the use of evolution under quadrupolar interaction for implementation of such algorithms. The Hamiltonian of Eq. (1) has two parts: (i) The Zeeman part $(\omega_0 I_z)$ and (ii) scaled quadrupolar part $[\Lambda(3I_z^2-I^2)]$. The pulse sequence $\tau/2-(\pi)-\tau/2$ focuses the Zeeman interaction but allows the system to evolve under the quadrupolar interaction. Similar to J coupling, quadrupolar coupling provides interaction among multiple qu-

TABLE I. Constant and balanced one-qubit functions.

	Constant		Balanced	
x	f_1	f_2	f_3	f_4
0	0	1	0	1
1	0	1	1	0

bits, and can be used by such sequences to implement multiqubit gates. Since the gate time is inversely proportional to the strength of the interaction, and the scaled quadrupolar coupling is three orders of magnitude greater than J coupling, the gate time decreases, thereby increasing, the clock speed of the quantum computer. However, in such systems the relaxation times are also smaller by two orders. Thus decoherence takes away some of the advantage of faster gate speeds. We have experimentally implemented DJ algorithm using quadrupolar coupling in ^{23}Na (spin-$\frac{3}{2}$) nuclei.

II. DEUTSCH-JOZSA ALGORITHM

The DJ algorithm determines the type of an unknown function when it is either constant or balanced. In the simplest case, $f(x)$ maps a single bit to a single bit. The function is called constant if $f(x)$ is independent of x and it is balanced if $f(x)$ is zero for one value of x and unity for the other value. For an N-qubit system, $f(x_1,x_2,\ldots,x_N)$ is constant if it is independent of x_i and balanced if it is zero for half the values of x_i and unity for the other half. Classically it requires $(2^{N-1}+1)$ function calls to check whether $f(x_1,x_2,\ldots,x_N)$ is constant or balanced. However the DJ algorithm would require only a single function call [1,2]. The Cleve version of the DJ algorithm implemented by using a unitary transformation by the propagator U_f while adding an extra qubit, is given by [27]

$$|x_1,x_2,\ldots,x_N\rangle|x_{N+1}\rangle \overset{U_f}{\rightarrow} |x_1,x_2,\ldots,x_N\rangle|x_{N+1} \oplus f(x_1,x_2,\ldots,x_N)\rangle. \quad (2)$$

The four possible functions for the single-bit DJ algorithm are given in Table I.

The unitary transformations corresponding to the four possible propagators U_f are

$$U_1=\begin{pmatrix}1&0&0&0\\0&1&0&0\\0&0&1&0\\0&0&0&1\end{pmatrix}, \quad U_2=\begin{pmatrix}0&1&0&0\\1&0&0&0\\0&0&0&1\\0&0&1&0\end{pmatrix},$$

$$U_3=\begin{pmatrix}1&0&0&0\\0&1&0&0\\0&0&0&1\\0&0&1&0\end{pmatrix}, \quad U_4=\begin{pmatrix}0&1&0&0\\1&0&0&0\\0&0&1&0\\0&0&0&1\end{pmatrix}. \quad (3)$$

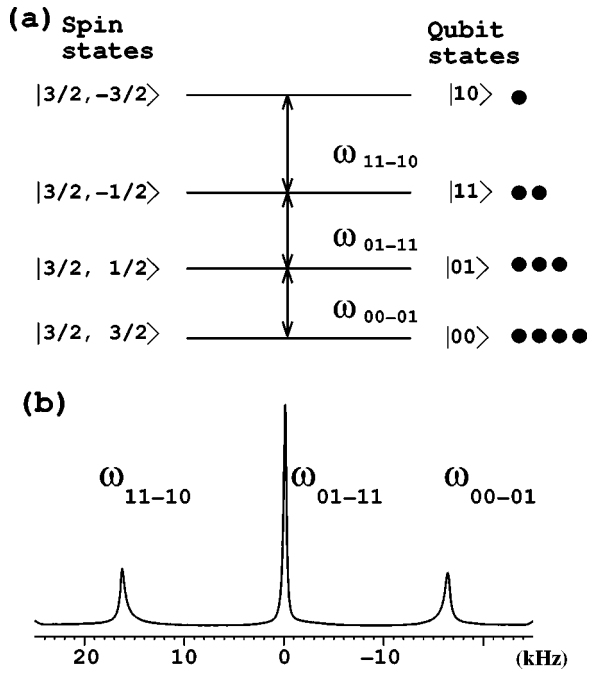

FIG. 1. (a) Energy level diagram of a spin-$\frac{3}{2}$ nucleus oriented in a liquid-crystal matrix. The different spin states can be labeled as states of a two-qubit system. The equilibrium deviation populations of different states under high-field high-temperature approximation are schematically shown by the dots on the right-hand side. (b) The equilibrium spectrum of ^{23}Na obtained after a hard $(\pi/2)_y$ pulse. Along x axis are the frequencies in kHz and along y axis are the intensities. The three single quantum transitions are well separated by an effective quadrupolar coupling Λ of about 16 kHz. The outer lines are broader than the inner line (linewidths are different due to differences in relaxation matrix elements as well as due to fluctuations in S values). These fluctuations in S values affect only the outer transitions in the first order, reducing their transverse relaxation time T_2. The integrated intensities are in the correct ratio of 3:4:3. The spectrum is plotted with a Lorentzian line-broadening factor of 200 Hz.

In the case of two qubits, there are two constant and six balanced functions. For higher qubits the functions are easy to evaluate using Eq. (2).

III. DJ ALGORITHM IN A SPIN-3/2 SYSTEM

The Cleve version of the algorithm implemented here requires two qubits: an input qubit and a work qubit [27]. Previous workers have demonstrated the algorithm using two weakly coupled spin-$\frac{1}{2}$ nuclei [10,11,13]. Here we implement it on a spin-$\frac{3}{2}$ nucleus. The energy level diagram of a spin-$\frac{3}{2}$ nucleus corresponding to the Hamiltonian of Eq. (4) is shown in Fig. 1(a). The four energy levels are labeled as levels of a two-qubit system [Fig. 1(a)]. There are three single quantum transitions among the four levels, labeled as ω_{00-01}, ω_{01-11} and ω_{11-10}, Fig. 1(b) (the subscript denotes the energy levels between which the transition takes place). While the above three transitions are single quantum trans-

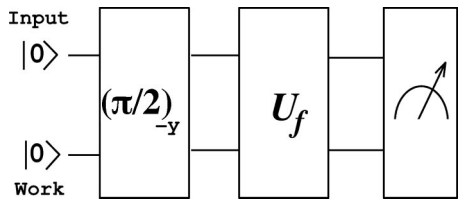

FIG. 2. Quantum circuit for implementing Deutsch-Jozsa algorithm. The first $(\pi/2)_{-y}$ hard pulse creates superposition of all states. U_f is the unitary transform corresponding to the function *f*. The last step is the measurement. In NMR this step can be simplified to acquisition of signal immediately after U_f is implemented. The sign of the input qubit's resonances with respect to those of the work qubits resonances [Eq. (6)] distinguishes between the constant and balanced functions.

tions ($\Delta m = \pm 1$) they are also single-qubit flip transitions. However, according to the present labeling scheme the single-qubit flip corresponding to $|00\rangle \leftrightarrow |10\rangle$ is a forbidden $\Delta m = \pm 3$ transition. The above labeling scheme was chosen to optimize the experimental implementation of the algorithm. As demonstrated in $I = 7/2$ systems elsewhere, optimum labeling schemes can be chosen for given logical operations [25].

The quantum circuit for implementation of the DJ algorithm followed in this work (Fig. 2) is similar to those used by previous workers [10,11]. The first qubit is the input qubit whereas the second qubit is the work qubit. The algorithm starts from a pure state $|\psi\rangle = |00\rangle$ followed by a Hadamard transform [11]. A pseudo-Hadamard operation can be implemented by using a high-power, low-duration ''hard'' $(\pi/2)$ pulse along the $(-y)$ axis which creates superposition of all the qubits [10,11]. In the spin-$\frac{3}{2}$ system the operator of hard $(\pi/2)_{-y}$ pulse is of the form

$$\exp(iI_y\pi/2) = \frac{1}{2\sqrt{2}}\begin{pmatrix} 1 & \sqrt{3} & \sqrt{3} & 1 \\ -\sqrt{3} & -1 & 1 & \sqrt{3} \\ \sqrt{3} & -1 & -1 & \sqrt{3} \\ -1 & \sqrt{3} & -\sqrt{3} & 1 \end{pmatrix}, \quad (4)$$

where the *y* component of spin angular momentum in the spin-$\frac{3}{2}$ system is

$$I_y = i\begin{pmatrix} 0 & -\sqrt{3}/2 & 0 & 0 \\ \sqrt{3}/2 & 0 & -1 & 0 \\ 0 & 1 & 0 & -\sqrt{3}/2 \\ 0 & 0 & \sqrt{3}/2 & 0 \end{pmatrix}. \quad (5)$$

The state of the system after $(\pi/2)_{-y}$ pulse is $|\psi'\rangle = \exp(iI_y\pi/2)|\psi\rangle = 1/2\sqrt{2}[|00\rangle - \sqrt{3}|01\rangle + \sqrt{3}|11\rangle - |10\rangle] = 1/2\sqrt{2}[(|0\rangle - |1\rangle)(|0\rangle - \sqrt{3}|1\rangle)]$.

It is to be noted that unlike weakly coupled spin-$\frac{1}{2}$ nuclei, the operator of $(\pi/2)_{-y}$ pulse used here does not create uniform superposition. However, it does create a coherent superposition of all the states which can be utilized for ''quantum parallelism'' as desired by the algorithm. This also works for higher-spin systems such as spin-$\frac{7}{2}$ nuclei which can act as a three-qubit system [28]. After creation of $|\psi'\rangle$ we apply the unitary operator U_f which yields $|\psi''_f\rangle = U_f|\psi'\rangle$. The operator U_1 is unity operator, yielding $|\psi''_1\rangle = U_1|\psi'\rangle = 1/2\sqrt{2}[(|0\rangle - |1\rangle)(|0\rangle - \sqrt{3}|1\rangle)]$. The operator U_2 flips the state of the second qubit, yielding $|\psi''_2\rangle = U_2|\psi'\rangle = 1/2\sqrt{2}[(|0\rangle - |1\rangle)(-\sqrt{3}|0\rangle + |1\rangle)]$. U_3 flips the state of the second qubit only when the state of the first qubit is $|1\rangle$ and U_4 flips the state of the second qubit only when the state of the first qubit is $|0\rangle$ (Table II). The operators U_3 and U_4 are thus controlled-NOT gates. It may be noted that similar to spin-$\frac{1}{2}$ case, the information about the function is encoded in the relative phase of the two states of the input qubit; (-1) for constant and $(+1)$ for balanced functions (Table II).

Density matrices of the system confirm the different functions. The density matrices corresponding to the states $|\psi''_f\rangle$ are σ''_f, given by

TABLE II. The function *f*, operator U_f, and wave function $|\psi''_f\rangle$ for one-qubit DJ.

Function *f*	Operator U_f	Wave function $\lvert\psi''_f\rangle$
f_1	U_1	$\frac{1}{2\sqrt{2}}[(\lvert0\rangle - \lvert1\rangle)(\lvert0\rangle - \sqrt{3}\lvert1\rangle)]$
f_2	U_2	$\frac{1}{2\sqrt{2}}[(\lvert0\rangle - \lvert1\rangle)(-\sqrt{3}\lvert0\rangle + \lvert1\rangle)]$
f_3	U_3	$\frac{1}{2\sqrt{2}}[(\lvert0\rangle + \sqrt{3}\lvert1\rangle)\lvert0\rangle - (\sqrt{3}\lvert0\rangle + \lvert1\rangle)\lvert1\rangle]$
f_4	U_4	$\frac{1}{2\sqrt{2}}[-(\sqrt{3}\lvert0\rangle + \lvert1\rangle)\lvert0\rangle + (\lvert0\rangle + \sqrt{3}\lvert1\rangle)\lvert1\rangle]$

$$\sigma_1''=\begin{pmatrix} |00\rangle & |01\rangle & |11\rangle & |10\rangle \\ 1 & -\sqrt{3} & \sqrt{3} & -1 \\ -\sqrt{3} & 3 & -3 & \sqrt{3} \\ \sqrt{3} & -3 & 3 & -\sqrt{3} \\ -1 & \sqrt{3} & -\sqrt{3} & 1 \end{pmatrix} \begin{matrix} |00\rangle \\ |01\rangle \\ |11\rangle \\ |10\rangle \end{matrix}, \quad \sigma_2''=\begin{pmatrix} 3 & -\sqrt{3} & \sqrt{3} & -3 \\ -\sqrt{3} & 1 & -1 & \sqrt{3} \\ \sqrt{3} & -1 & 1 & -\sqrt{3} \\ -3 & \sqrt{3} & -\sqrt{3} & 3 \end{pmatrix},$$

$$\sigma_3''=\begin{pmatrix} 3 & -\sqrt{3} & -3 & \sqrt{3} \\ -\sqrt{3} & 1 & \sqrt{3} & -1 \\ -3 & \sqrt{3} & 3 & -\sqrt{3} \\ \sqrt{3} & -1 & -\sqrt{3} & 1 \end{pmatrix}, \quad \sigma_4''=\begin{pmatrix} 1 & -\sqrt{3} & -1 & \sqrt{3} \\ -\sqrt{3} & 3 & \sqrt{3} & -3 \\ -1 & \sqrt{3} & 1 & -\sqrt{3} \\ \sqrt{3} & -3 & -\sqrt{3} & 3 \end{pmatrix}. \tag{6}$$

The signs of input qubit coherences $|11\rangle \leftrightarrow |01\rangle$ and $|10\rangle \leftrightarrow |00\rangle$ are negative for σ_1'' and σ_2'' but positive for σ_3'' and σ_4'', indicating, respectively, constant and balanced functions.

After U_f, one needs to make a measurement (Fig. 2). Theoretically this step needs a Hadamard gate followed by a readout of input qubit. In NMR, the Hadamard is replaced by a pseudo-Hadamard, which can be implemented by a $(\pi/2)$ pulse. Similarly, the readout is also another $(\pi/2)$ pulse. These two pulses cancel each other and hence in NMR the result of DJ algorithm is directly available after implementation of U_f [11]. As seen from Eq. (6), in the signal acquired immediately following U_f, the resonance of the input qubit at ω_{01-11} (the central transition of Fig. 1) will be of the same sign as the resonances of the work qubit at ω_{00-01} and ω_{11-10} (the outer transitions of Fig. 1) for constant functions, and of opposite sign for the balanced functions. It may be mentioned that only one of the transitions of the input qubit, namely, $|01\rangle \leftrightarrow |11\rangle$ is observed here, the other transition $|00\rangle \leftrightarrow |10\rangle$ being $\Delta m = \pm 3$.

IV. EXPERIMENT

The DJ algorithm is experimentally implemented here on ^{23}Na (spin-$\frac{3}{2}$) nuclei of a lyotropic liquid crystal composed of 37.9% sodium dodecyl sulfate, 6.7% decanol, and 55.4% water. The liquid crystal had a nematic phase at 299 K [21,31]. All experiments were performed on a DRX 500 MHz spectrometer. Figure 1(b) shows the equilibrium spectrum consisting of three lines, with an effective quadrupolar coupling Λ of about 16 kHz and integrated intensity ratio 3:4:3.

The $|00\rangle$ pseudopure state is created by applying a selective population inversion (π) pulse on the $|10\rangle \leftrightarrow |11\rangle$ transition followed by a population equilibration $(\pi/2)$ pulse on $|01\rangle \leftrightarrow |11\rangle$ transition and a gradient pulse to kill created coherences [9,24]. Transition selective pulses are long-duration, low-power rf pulses applied at the resonant frequency between two energy levels, which excite a selected transition of the spectrum and leave the others unperturbed. Let us consider a two-level subsystem $|i\rangle$ and $|j\rangle$, whose equilibrium deviation populations are p_i and p_j,

$$\sigma=\begin{pmatrix} p_i & 0 \\ 0 & p_j \end{pmatrix}. \tag{7}$$

The operator of a transition selective (θ) pulse about the y axis between these two levels would be

$$\exp(-iI_y^{|i\rangle\leftrightarrow|j\rangle}\theta)=\begin{pmatrix} \cos(\theta/2) & \sin(\theta/2) \\ -\sin(\theta/2) & \cos(\theta/2) \end{pmatrix}, \tag{8}$$

where the angular-momentum operator

$$I_y^{|i\rangle\leftrightarrow|j\rangle}=\begin{pmatrix} 0 & -i \\ i & 0 \end{pmatrix}.$$

A population inversion (π) pulse will interchange the populations between the two levels,

$$\exp(-iI_y^{|i\rangle\leftrightarrow|j\rangle}\pi)\sigma\exp(iI_y^{|i\rangle\leftrightarrow|j\rangle}\pi) = \begin{pmatrix} 0 & 1 \\ -1 & 0 \end{pmatrix}\begin{pmatrix} p_i & 0 \\ 0 & p_j \end{pmatrix}\begin{pmatrix} 0 & -1 \\ 1 & 0 \end{pmatrix}=\begin{pmatrix} p_j & 0 \\ 0 & p_i \end{pmatrix}. \tag{9}$$

A population equilibration $(\pi/2)$ pulse will equilibrate the populations and create coherences of the form

$$\exp(-iI_y^{|i\rangle\leftrightarrow|j\rangle}\pi/2)\sigma\exp(iI_y^{|i\rangle\leftrightarrow|j\rangle}\pi/2) = \frac{1}{\sqrt{2}}\begin{pmatrix} 1 & 1 \\ -1 & 1 \end{pmatrix}\begin{pmatrix} p_i & 0 \\ 0 & p_j \end{pmatrix}\frac{1}{\sqrt{2}}\begin{pmatrix} 1 & -1 \\ 1 & 1 \end{pmatrix} = \begin{pmatrix} (p_i+p_j)/2 & (p_j-p_i)/2 \\ (p_j-p_i)/2 & (p_i+p_j)/2 \end{pmatrix}, \tag{10}$$

which followed by gradient will retain the populations but destroy the coherences.

After the creation of a pseudopure state the coherent superposition of both the qubits are created by a nonselective $(\pi/2)_{-y}$ pulse. At this stage one can apply the various U_f. The function U_1 needs no pulse and the result given in Fig.

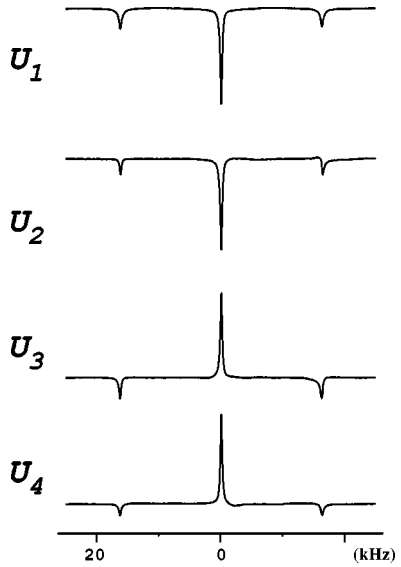

FIG. 3. Implementation of DJ algorithm on ^{23}Na (spin-$\frac{3}{2}$) nuclei. The algorithm starts from $|00\rangle$ pseudopure state. After running through the quantum circuit of Fig. 1, the acquired signal is Fourier transformed. The spectra corresponding to the operations U_1, U_2, U_3, and U_4 are given. Along x axis are the frequencies in kHz and along y axis are the intensities. Constant functions are distinguished from balanced functions by the sign of resonance of the input qubit. As seen by the single quantum coherences of Eq. (6), for U_1 and U_2 the resonance of input qubit (central transition) has same sign as the resonances of the work qubit (outer transitions), implying that the corresponding functions f_1 and f_2 are constant; whereas for U_3 and U_4, the sign of the central transition are opposite, indicating that f_3 and f_4 are balanced.

3 indicates that all the three transitions are of same sign and hence it is a constant function. The operator U_2 in Eq. (3) requires two transition selective pulses $(\pi/\sqrt{3})_x^{|00\rangle\leftrightarrow|01\rangle}(\pi/\sqrt{3})_x^{|10\rangle\leftrightarrow|11\rangle}$, where,

$$(\pi/\sqrt{3})_x^{|00\rangle\leftrightarrow|01\rangle}(\pi/\sqrt{3})_x^{|10\rangle\leftrightarrow|11\rangle}=\begin{pmatrix}0&i&0&0\\ i&0&0&0\\ 0&0&0&i\\ 0&0&i&0\end{pmatrix}=i\begin{pmatrix}0&1&0&0\\ 1&0&0&0\\ 0&0&0&1\\ 0&0&1&0\end{pmatrix}. \tag{11}$$

Here we have used the fact that

$$(\theta)_x^{|00\rangle\leftrightarrow|01\rangle}=\exp(iI_x^{00\leftrightarrow01}\theta)=\begin{pmatrix}\cos(\sqrt{3}\theta/2)&i\sin(\sqrt{3}\theta/2)&0&0\\ i\sin(\sqrt{3}\theta/2)&\cos(\sqrt{3}\theta/2)&0&0\\ 0&0&1&0\\ 0&0&0&1\end{pmatrix},$$

$$(\theta)_x^{|10\rangle\leftrightarrow|11\rangle}=\exp(iI_x^{10\leftrightarrow11}\theta)=\begin{pmatrix}1&0&0&0\\ 0&1&0&0\\ 0&0&\cos(\sqrt{3}\theta/2)&i\sin(\sqrt{3}\theta/2)\\ 0&0&i\sin(\sqrt{3}\theta/2)&\cos(\sqrt{3}\theta/2)\end{pmatrix}. \tag{12}$$

The result given in Fig. 3 confirms that f_2 is also a constant function. While implementing U_3 of Eq. (3) we note that the Pound-Overhauser controlled-NOT gate [8] is similar to U_3, but differs from its exact form by a controlled phase operator

$$U_3=\begin{pmatrix}1&0&0&0\\ 0&1&0&0\\ 0&0&0&1\\ 0&0&-1&0\end{pmatrix}\begin{pmatrix}1&0&0&0\\ 0&1&0&0\\ 0&0&e^{i\pi}&0\\ 0&0&0&1\end{pmatrix}. \tag{13}$$

The Pound-Overhauser controlled-NOT gate is implemented by a transition selective $(\pi/\sqrt{3})_{-y}^{|10\rangle\leftrightarrow|11\rangle}$ pulse. The controlled phase shift operator of Eq. (13) can be realized by using (i) only transition selective pulses or (ii) transition selective pulses along with a evolution under quadrupolar coupling.

(i) Transition selective pulse method. Transition selective z pulses can be used to introduce specific phases to the different states [30]. For example, the $(\phi)_z^{01\leftrightarrow11}$ introduces a phase shift of 2ϕ between the states $|01\rangle$ and $|11\rangle$. $(\phi)_z^{01\leftrightarrow11}$ is implemented using three selective pulses $(\pi/4)_y(\phi)_x(\pi/4)_{-y}$ on the transition $|01\rangle\leftrightarrow|11\rangle$:

$$(\phi)_z^{01\leftrightarrow11}=\exp(-iI_y^{01\leftrightarrow11}\pi/4)\times\exp(-iI_x^{01\leftrightarrow11}\phi)\exp(iI_y^{01\leftrightarrow11}\pi/4)=\begin{pmatrix}1&0&0&0\\ 0&e^{-i\phi}&0&0\\ 0&0&e^{i\phi}&0\\ 0&0&0&1\end{pmatrix}, \tag{14}$$

where the x and y components of the operator of transition between the states $|01\rangle\leftrightarrow|11\rangle$ are

$$I_x^{01\leftrightarrow11}=\begin{pmatrix}0&0&0&0\\ 0&0&1&0\\ 0&1&0&0\\ 0&0&0&0\end{pmatrix},\quad I_y^{01\leftrightarrow11}=\begin{pmatrix}0&0&0&0\\ 0&0&-i&0\\ 0&i&0&0\\ 0&0&0&0\end{pmatrix}. \tag{15}$$

Hence the controlled phase shift operator of Eq. (13) can be achieved by using a cascade of three transition selective z pulses

$$(\pi/4)_z^{|00\rangle\leftrightarrow|01\rangle}(\pi/4)_z^{|10\rangle\leftrightarrow|11\rangle}(\pi/2)_z^{|01\rangle\leftrightarrow|11\rangle}=\begin{pmatrix} e^{-i\pi/4} & 0 & 0 & 0 \\ 0 & e^{i\pi/4} & 0 & 0 \\ 0 & 0 & 1 & 0 \\ 0 & 0 & 0 & 1 \end{pmatrix}\begin{pmatrix} 1 & 0 & 0 & 0 \\ 0 & 1 & 0 & 0 \\ 0 & 0 & e^{i\pi/4} & 0 \\ 0 & 0 & 0 & e^{-i\pi/4} \end{pmatrix}\begin{pmatrix} 1 & 0 & 0 & 0 \\ 0 & e^{-i\pi/2} & 0 & 0 \\ 0 & 0 & e^{i\pi/2} & 0 \\ 0 & 0 & 0 & 1 \end{pmatrix}$$

$$=e^{-i\pi/4}\begin{pmatrix} 1 & 0 & 0 & 0 \\ 0 & 1 & 0 & 0 \\ 0 & 0 & e^{i\pi} & 0 \\ 0 & 0 & 0 & 1 \end{pmatrix}. \tag{16}$$

(ii) Evolution under quadrupolar coupling method. Similar to *J* coupling, evolution under the quadrupolar coupling rotates the system about the *z* axis, introducing specific phases to the states. The quadrupolar Hamiltonian in the spin-$\frac{3}{2}$ system is of the form

$$\mathcal{H}_Q=\Lambda(3Iz^2-I^2)=3\Lambda\begin{pmatrix} 1 & 0 & 0 & 0 \\ 0 & -1 & 0 & 0 \\ 0 & 0 & -1 & 0 \\ 0 & 0 & 0 & 1 \end{pmatrix}. \tag{17}$$

The operator corresponding to evolution under the quadrupolar Hamiltonian for a time τ is

$$e^{i\mathcal{H}_Q\tau}=\exp[-i\Lambda(3Iz^2-I^2)\tau]$$

$$=\begin{pmatrix} e^{-i3\Lambda\tau} & 0 & 0 & 0 \\ 0 & e^{i3\Lambda\tau} & 0 & 0 \\ 0 & 0 & e^{i3\Lambda\tau} & 0 \\ 0 & 0 & 0 & e^{-i3\Lambda\tau} \end{pmatrix}. \tag{18}$$

Hence the controlled phase shift operator of Eq. (13) can be achieved by a combination $(e^{i\mathcal{H}_Q\tau})(\pi/2)_z^{01\leftrightarrow 11}$, where $\tau=\pi/12\Lambda$ is the time period of evolution under the quadrupolar Hamiltonian.

We have implemented approach (ii) in our experiments. This is because, the use of evolution under quadrupolar coupling reduces the number of transition selective pulses, enabling fast computation and less errors due to relaxation. All the experiments were carried out with the carrier frequency of the rf pulses matching with the central transition (on-resonance). In this situation, the evolution in the rotating frame takes place only under quadrupolar Hamiltonian and the Zeeman term does not evolve. U_3 was implemented by a pulse sequence

$$(\pi/\sqrt{3})_{-y}^{|10\rangle\leftrightarrow|11\rangle}(e^{i\mathcal{H}_Q\tau})(\pi/2)_z^{|01\rangle\leftrightarrow|11\rangle}=\begin{pmatrix} 1 & 0 & 0 & 0 \\ 0 & 1 & 0 & 0 \\ 0 & 0 & 0 & 1 \\ 0 & 0 & -1 & 0 \end{pmatrix}\begin{pmatrix} e^{-i\pi/4} & 0 & 0 & 0 \\ 0 & e^{i\pi/4} & 0 & 0 \\ 0 & 0 & e^{i\pi/4} & 0 \\ 0 & 0 & 0 & e^{-i\pi/4} \end{pmatrix}\begin{pmatrix} 1 & 0 & 0 & 0 \\ 0 & e^{-i\pi/2} & 0 & 0 \\ 0 & 0 & e^{i\pi/2} & 0 \\ 0 & 0 & 0 & 1 \end{pmatrix}$$

$$=\begin{pmatrix} 1 & 0 & 0 & 0 \\ 0 & 1 & 0 & 0 \\ 0 & 0 & 0 & 1 \\ 0 & 0 & -1 & 0 \end{pmatrix}e^{-i\pi/4}\begin{pmatrix} 1 & 0 & 0 & 0 \\ 0 & 1 & 0 & 0 \\ 0 & 0 & e^{i\pi} & 0 \\ 0 & 0 & 0 & 1 \end{pmatrix}=e^{-i\pi/4}\begin{pmatrix} 1 & 0 & 0 & 0 \\ 0 & 1 & 0 & 0 \\ 0 & 0 & 0 & 1 \\ 0 & 0 & 1 & 0 \end{pmatrix}, \tag{19}$$

where $\tau=\pi/12\Lambda$. The operator U_4 was implemented by a similar pulse sequence $(\pi/\sqrt{3})_{-y}^{|00\rangle\leftrightarrow|01\rangle}(e^{i\mathcal{H}_Q\tau})(\pi/2)_{-z}^{|00\rangle\leftrightarrow|01\rangle}$, with the same value of τ. The result after applying U_3 and U_4 is given in Fig. 3, in which it is seen that the sign of central transition is opposite to that of the outer transitions, indicating that f_3 and f_4 are balanced functions [Eq. (6)].

The selective excitation in this paper is achieved using Gaussian soft pulses [32] of length 123 μs. During the selective pulses the unexcited transitions continue to experience quadrupolar interaction, resulting in a rotation around the z axis, which leads to phase errors. To minimize such errors, the lengths of the selective pulses were so chosen that the phase rotation is in multiples of 2π [11]. However, errors due to relaxation could not be avoided. For example, the peak intensities are slightly different from the expected. It is because the relaxation times are $T_1=16$ ms for all the three transitions, $T_2=14$ ms for the central transition, and 4 ms for the outer transitions. Since, the relaxation time of the outer transitions is less than the central, the coherences of the outer transitions decay faster, decreasing their peak intensities.

In quantum-information processing by NMR, the gate time is of the order of the inverse of coupling and the coherence time is proportional to the inverse of the linewidth. In liquids the coupling values are $\sim$100 Hz and the linewidth $\sim$1 Hz yielding a gate time $\sim$3 ms, a coherence time $\sim$300 ms and hence a dynamic range of two orders of magnitude. In the quadrupolar system described in this paper, the quadrupolar coupling value is $\sim$16 kHz yielding an evolution time $\sim$20 μs. Since the coherence times are 14 ms and 4 ms for inner and outer transitions, respectively, the system yields a dynamic range of three orders of magnitude. Thus, both the dynamic range and the clock speed (inverse of gate time) are better in the quadrupolar system described here.

V. CONCLUSIONS

The implementation of quantum algorithms on quadrupolar nuclei validate their use as an alternate candidate for quantum-information processing. The DJ algorithm has been implemented here in a spin-$\frac{3}{2}$ system by manipulation of coherent superposition using evolution under quadrupolar interaction and rf pulses. The errors in our experiments were mainly caused by relaxation and imperfection of rf pulses. Use of tailored multifrequency pulses [22] can further decrease gate time and relaxation errors. Some quantum algorithms such as Grover's search algorithm require uniform superposition of states, which can be realized by application of multiple quantum pulses [29]. Efforts are ongoing in our lab to develop such pulses and implement various quantum algorithms in $\frac{3}{2}$ and $\frac{7}{2}$ spin systems. Since completion of this work, an implementation of continuous version of Grover's search algorithm [33], and creation of pseudopure states and entangled states in the solid state [34], have been reported in spin-$\frac{3}{2}$ systems.

ACKNOWLEDGMENTS

The authors thank T.S. Mahesh, Neeraj Sinha, N. Suryaprakash, and K.V. Ramanathan for useful discussions. The use of DRX-500 NMR spectrometer funded by the Department of Science and Technology, New Delhi, at the Sophisticated Instruments. Facility, Indian Institute of Science, Bangalore, is also gratefully acknowledged.

[1] D. Deutsch, Proc. R. Soc. London, Ser. A **400**, 97 (1985).
[2] D. Deutsch and R. Jozsa, Proc. R. Soc. London, Ser. A **493**, 553 (1992).
[3] *The Physics of Quantum Information*, edited by D. Bouwmeester, A. Ekert, and A. Zeilinger (Springer, Berlin, 2000).
[4] M.A. Nielsen and I.L. Chuang, *Quantum Computation and Quantum Information* (Cambridge University Press, Cambridge, UK, 2000).
[5] P.W. Shor, SIAM Rev. **41**, 303 (1999).
[6] L.K. Grover, Phys. Rev. Lett. **79**, 325 (1997).
[7] N.A. Gershenfeld and I.L. Chuang, Science **275**, 350 (1997).
[8] D.G. Cory, M.D. Price, and T.F. Havel, Physica D **120**, 82 (1997).
[9] Z.L. Madi, R. Bruschweiler, and R.R. Ernst, J. Chem. Phys. **109**, 10603 (1998).
[10] I.L. Chuang, L.M.K. Vanderspyen, X. Zhou, D.W. Leung, and S. Lloyd, Nature (London) **393**, 1443 (1998).
[11] J.A. Jones and M. Mosca, J. Chem. Phys. **109**, 1648 (1998).
[12] N. Lindan, H. Barjat, and R. Freeman, Chem. Phys. Lett. **296**, 61 (1998).
[13] Kavita Dorai, Arvind, and Anil Kumar, Phys. Rev. A **61**, 042306 (2000).
[14] T.S. Mahesh, Kavita Dorai, Arvind, and Anil Kumar, J. Magn. Reson. **148**, 95 (2001).
[15] I.L. Chuang, N. Gershenfeld, and M. Kubinec, Phys. Rev. Lett. **80**, 3408 (1998).
[16] J.A. Jones, M. Mosca, and R.H. Hansen, Nature (London) **393**, 344 (1998).
[17] L.M.K. Vanderspypen, M. Steffen, M.H. Sherwood, C.S. Yannoni, R. Cleve, and I.L. Chuang, Appl. Phys. Lett. **76**, 646 (2000).
[18] L.M.K. Vanderspyen, Matthias Steffen, Gregory Breyta, C.S. Yannoni, M.H. Sherwood and I.L. Chuang, Nature (London) **414**, 883 (2001).
[19] J.A. Jones, Prog. Nucl. Magn. Reson. Spectrosc. **38**, 325 (2001).
[20] D.G. Cory *et al.*, e-print quant-ph/0004104 (2000).
[21] A.K. Khitrin and B.M. Fung, J. Chem. Phys. **112**, 6963 (2000).
[22] A. Khitrin, H. Sun, and B.M. Fung, Phys. Rev. A **63**, 020301(R) (2001).
[23] A.K. Khitrin and B.M. Fung, Phys. Rev. A **64**, 032306 (2001).
[24] Neeraj Sinha, T.S. Mahesh, K.V. Ramanathan, and Anil Kumar, J. Chem. Phys. **114**, 4415 (2002).
[25] K.V.R.M. Murali, Neeraj Sinha, T.S. Mahesh, Malcom Levitt, K.V. Ramanathan, and Anil Kumar, Phys. Rev. A **66**, 022313 (2002).
[26] P. Dhiel and C.L. Khetrapal, *NMR-Basic Principles and Progress* (Springer-Verlag, New York, 1969), Vol. 1.

[27] R. Cleve, A. Ekert, C. Macchiavello, and M. Mosca, Proc. R. Soc. London, Ser. A **454**, 339 (1998).
[28] Ranabir Das and Anil Kumar, in *9th National Magnatic Resonance Symposium* (Indian Institute of Science, Bangalore, 2003).
[29] S. Vega, J. Chem. Phys. **68**, 5518 (1978).
[30] Ranabir Das, T.S. Mahesh, and Anil Kumar, J. Magn. Reson. **159**, 46 (2002).
[31] K. Radley, L.W. Reeves, and A.S. Tracey, J. Chem. Phys. **80**, 174 (1976).
[32] C.J. Bauer, R. Freeman, T. Frenkiel, J. Keeler, and A.J. Shaka, J. Magn. Reson. **58**, 442 (1984).
[33] V.L. Ermakov and B.M. Fung, Phys. Rev. A **66**, 042310 (2002).
[34] H. Kampermann and W.S. Veeman, Quantum Inf. Process. **1**, 327 (2002).